https://dx.doi.org/10.21577/0103-5053.20220049

J. Braz. Chem. Soc., Vol. 33, No. 8, 958-968, 2022

Article

On-line Micro-Packed Column Solid-Phase Extraction of Cadmium Using Metal-Organic Framework (MOF) UiO-66 with Posterior Determination by TS-FF-AAS

Ana Carla R. Carneiro,[a] Joziane G. Meneguin,[a] Paula M. dos Santos,[a] Marcela Z. Corazza,[a] Maiyara Carolyne Prete,[a] Andrelson Wellington Rinaldi[b] and César Ricardo T. Tarley[*,a,c]

[a]Departamento de Química, Universidade Estadual de Londrina, Rodovia Celso Garcia Cid, PR 445 Km 380, Campus Universitário, 86051-990 Londrina-PR, Brazil

[b]Departamento de Química, Universidade Estadual de Maringá, Av. Colombo, Campus Universitário, 87020-900 Maringá-PR, Brazil

[c]Departamento de Química Analítica, Instituto de Química, Instituto Nacional de Ciência e Tecnologia em Bioanalítica (INCT-BIO), Universidade Estadual de Campinas, (UNICAMP), Cidade Universitária Zeferino Vaz, 13083-970 Campinas-SP, Brazil

Metal-organic framework (MOF) UiO-66 was synthesized and evaluated as solid-phase extractor support for cadmium preconcentration in a micro-flow injection system coupled to thermospray flame furnace atomic absorption spectrometry (TS-FF-AAS) detection. The adsorbent was characterized by X-ray diffraction, Fourier transform infrared spectroscopy (FTIR), scanning electron microscopy (SEM), Raman spectroscopy, and textural data from N_2 adsorption/desorption isotherm data. The optimized conditions were achieved by loading 10.0 mL of a sample, containing 0.05 mol L^{-1} of phosphate buffer solution at pH 8.0, at a high flow rate of 10.0 mL^{-1} through 20.0 mg of UiO-66 packed into a mini-column, followed by elution with 1.0 mol L^{-1} HCl. At these conditions, the method presented a preconcentration factor of 35.7, limit of detection of 0.03 µg L^{-1} and a dynamic linear range from 0.1 to 8.0 µg L^{-1}. The adsorption performance of UiO-66 towards cadmium was not influenced by Pb^{2+}, Hg^{2+}, Fe^{2+}, Co^{2+}, Cu^{2+}, Ni^{2+}, Zn^{2+}, Mg^{2+} and Ca^{2+} ions. Analysis of different waters samples (tap water, physiological solution, mineral water, and lake water) was carried out without matrix interference, yielding recovery values ranging from 92.0 to 111.9%.

Keywords: FIA system, metal-organic framework, UiO-66, TS-FF-AAS, cadmium

Introduction

The presence of cadmium in the aquatic environment, represents, in general, a significant risk to aquatic biota and water quality due to its extremely long biological half-life and high toxicity. In humans, the ingestion of cadmium may cause renal abnormalities and nervous system diseases, apart from being considered a carcinogenic element.[1] The maximum allowed level of cadmium in drinking water has been established as 5.0 and 3.0 µg L^{-1} by the United States Environmental Protection Agency (USEPA)[2] and the World Health Organization (WHO)[3], respectively. In Brazil, the Ministry of Health also establishes the maximum of 3.0 µg L^{-1} of cadmium in drinking water.[4]

Cadmium determination in the µg L^{-1} concentration range is usually performed by graphite furnace atomic absorption spectrometry (GF AAS) and inductively coupled plasma mass spectrometry (ICP-MS). However, the acquisition and maintenance costs of these techniques are relatively expensive.[5] In turn, flame atomic absorption spectrometry (FAAS) stands out due to its easy operation and low cost of acquisition and maintenance. Nevertheless, the main drawback of this technique is its low sensitivity. Therefore, preconcentration methods prior to FAAS determination have been widely reported to improve the sensitivity.[6,7] Additionally, analytical strategies for sensitivity enhancement in FAAS based on total sample introduction[8] and atom-trapping techniques[9] to prolong the

*e-mail: tarley@uel.br
Editor handled this article: Luiz Ramos (Guest)

residence time of the analytes and higher atom absorption volume also has been investigated. The thermospray flame furnace atomic absorption spectrometry (TS-FF-AAS) technique, reported in 2000 by Gáspár and Berndt,[10] combine both features due to the efficiency of sample introduction into the Ni metallic atomizer placed on the burner head, and the confinement of atoms inside the flame furnace with prolonged residence time.

Within the framework of current green analytical chemistry requirements, with a particular emphasis on preconcentration methods, the dispersive micro-solid phase extraction (D-μSPE),[11] dispersive liquid-liquid microextraction (DLLME),[12] cloud point extraction (CPE),[13] supramolecular (SUPRA) solvent-based extraction[14] and micro-packed column flow solid-phase extraction[15] have been widely used. Although the first ones make use of microvolumes of elution solvent, microvolumes of extractor solvent, relatively non-toxic surfactants or carboxylic acid and alkanols-based extractors, the micro-packed column flow solid-phase extraction makes possible the use of large preconcentration volumes, thereby yielding high preconcentration factors, in addition of providing high sample throughput. Nevertheless, the criteria of green chemistry will only be attended by this solid-phase extraction method in flow analysis when ensuring the elimination or minimization of highly toxic chemical reagents, particularly toxic organic solvents and chelating agents in the flow system.[16] In this sense, the nature of adsorbents plays an important role in the performance of solid-phase extraction, in which the most desirable characteristics include large surface area, good chemical stability, high reusability and satisfactory selectivity. Carbonaceous nanomaterials, such as carbon nanotubes[17] and graphene[18] are great examples of adsorbents, however, their adsorptive performance depends on chemical or physical surface modification to provide selectivity and higher binding capacities towards metallic ions.

Metal-organic frameworks (MOFs) belong to a fascinating class of porous inorganic materials with widespread application including, for instance, catalysis, sensing, gas storage and separation science.[19] MOFs are defined as 3D coordination polymers formed by metal ions (or clusters) and multi-dentate organic ligands through coordination bonds. The metal substitution in this structure can directly alter the coordination units, creating new properties once it may cumulate different catalytically active sites and/or tune adsorptive, optoelectronic, and magnetic properties.[20] MOFs are named with an acronym representing the name where they were originally obtained or according to their framework, and the most common are MIL-n (MIL: Matériaux de I'Institut Lavoisier), HKUST-n (HKUST: Hong-Kong University of Science and Technology), UiO-n (UiO: Universitetet i Oslo) and ZIFs (zeolitic imidazolate frameworks). Some relevant properties of MOFs are ultrahigh surface area (1000-10400 $m^2\ g^{-1}$), ultra-low densities, crystalline open structure with tunable pore sizes, tailorable polarity, designable organic ligands, and high thermal stability (300-600 ºC).[21-24]

MOFs-based separation methods fulfill the aspects of green analytical chemistry due to the low-toxicity of metal ions used in MOFs synthesis, such as alkaline earth metals (Mg or Ca), or Mn, Fe, Al, Ti and Zr, attested by cytotoxicity studies, the absence of toxic chelating agents in the framework, the possibility of miniaturization in the separation process, as well as the absence of toxic organic solvent as eluent of metal ions.[19]

It has been observed an increasing trend in the research on the use of MOFs on the removal of heavy metals pollutants from water samples, as well as solid-phase extraction-based methods.[25,26] However, owing to their nanometer-size, MOFs have been mostly applied as adsorbents for metal ions in D-μSPE[24] or magnetic dispersive solid-phase extraction (MDSPE).[27] There are also applications of MOFs as adsorbents for on-line solid-phase extraction coupled to high performance liquid chromatography (HPLC)[28,29] and as monolithic column.[30] At the best of our knowledge, MOFs packed into closed mini-columns in flow systems for metal ions preconcentration has not been reported yet. This type of investigation is of paramount importance to assess the chemical stability, selectivity, and adsorption capacity of MOFs, since equilibrium and mass transfer kinetics is rather different from dispersive solid-phase extraction. Particularly in the case of MOFs, the selectivity towards a target metal ion depends on the flexibility of highly porous structure of the adsorbent, shape and size of the pores and the diffusion of analyte into the bulk structure, which is fully dependent on the hydrodynamic conditions of the packed mini-columns, such as the swelling effect and flow rate.

Therefore, in this work, UiO-66 was evaluated as adsorbent for the development of a novel on-line micro-packed column solid-phase extraction method coupled to TS-FF-AAS for cadmium determination in the μg L^{-1} concentration range in water samples. It is worth to emphasize that, due to the nanostructure of UiO-66, a very low amount of adsorbent can be used into the mini-column, which results in advantages in the on-line coupling with analytical techniques that works with low flow rates, such as TS-FF-AAS. UiO-66 was herein used since it is a well-known Zr-based cubic framework comprised of cationic $Zr_6O_4(OH)_4$ nodes and 1,4-benzene dicarboxylate organic linkers. Moreover, UiO-66 exhibits high chemical stability

in a variety of organic solvents, as well as acidic and basic aqueous media, besides its high surface area.[31-34]

Experimental

Reagents and instrumentation

All solutions were prepared using chemical reagents of analytical grade and ultrapure water from ELGA PURELAB Maxim system (High Wycombe, Bucks, UK), 18.2 MΩ cm resistivity. To prevent metal contamination, all glassware was kept overnight in a 10% (v/v) HNO_3 solution. Cd^{2+} working solutions at 5.0 μg L^{-1} were prepared from a 1000.0 mg L^{-1} Cd^{2+} standard stock solution (SpecSol®, Belo Horizonte, Brazil) by making appropriate dilutions. Phosphate buffer solutions were prepared by dissolving appropriate amounts of $NaH_2PO_4.H_2O$ (J. T. Baker®, Chicago, USA) in ultrapure water, without further purification, followed by pH adjustment to the desired value with sodium hydroxide and/or nitric acid (Vetec, Brazil) solutions. Zirconium(IV) oxychloride octahydrate and terephthalic acid used in the MOF synthesis were acquired from Sigma-Aldrich (Darmstadt, Germany), while *N*,*N*-dimethylformamide (DMF) was purchased from Synth (Diadema, Brazil) and hydrochloric acid (37%, v/v) was purchased from Sigma-Aldrich (Darmstadt, Germany). Solutions of Pb^{2+}, Fe^{2+}, Co^{2+}, Cu^{2+}, Ni^{2+}, Mg^{2+}, and Ca^{2+} used in interference studies were prepared from their respective nitrate salts, while the solution of Hg^{2+} was prepared from appropriate dilution of a standard stock solution at 1000.0 mg L^{-1} concentration (Specsol®, Belo Horizonte, Brazil).

The measurements were performed by using an AA-6601 flame atomic absorption spectrophotometer (Shimadzu, Kyoto, Japan) equipped with a cadmium hollow cathode lamp (Hamamatsu Photonics K.K., Hamamatsu City, Japan), operating at 8.0 mA and 228.8 nm, and a deuterium lamp for background correction. The flame composition was operated at an acetylene flow rate of 1.8 L min^{-1} and air flow rate of 15.0 L min^{-1}. For construction of the on-line preconcentration system coupled to TS-FF-AAS, a peristaltic pump (Gilson Minipuls Evolution, Middleton, USA), a home-made injector commutator made of Teflon® (PTFE, polytetrafluoroethylene), a 0.5 mm internal diameter (i.d.) ceramic capillary (Al_2O_3 99.7%) (Friatec, Germany), a 10 cm long and 2.5 cm i.d. nickel tube (72% of Ni, 14-17% of Cr, 6-10% of Fe, 0.15% of C, 1% of Mn and 0.5% of Si, Camacam, Brazil), containing 6 holes of 2.5 mm i.d. and Tygon® tubes were used. Figure S1 depicts the flow injection system coupled to TS-FF-AAS (Supplementary Information (SI) section).

The pH of samples was measured by an 826 pH mobile Metrohm pHmeter (Herisau, Switzerland). In order to identify the functional groups of the UiO-66 MOF, an infrared spectrometer with Fourier transform (FTIR, Bomem-Michelson, MB-100) operating in the transmission mode between 4000 and 400 cm^{-1} and using the KBr pellet method, was used. X-ray diffraction (XRD) spectra were acquired from a Shimadzu XRD-6000 X-ray diffractometer (Netherlands) operating with incident X-rays (Cu Kα of 1.54060 Å) with the 2θ angle between 5 and 40º, current of 40 mA and voltage of 40 kV. For scanning electron microscopy (SEM), analysis, the UiO-66 was coated with a thin layer of gold (30 nm) using Bal-Tec SCD Equipment Sputter Coater (New York, USA). The SEM UiO-66 images were obtained with magnification of 6000 and 50000 times with a range of 20.0 and 2.0 μm, respectively. The Raman spectra were obtained on a Raman Senterra microscope (Bruker©, Billerica, Massachusetts, USA), equipped with a 785 nm beam and a resolution of 3-5 cm^{-1}, operating in the spectral range from 70 to 3500 cm^{-1}. Nitrogen sorption/desorption experiments were performed on a Micromeritics (ASAP 2020) coupled to an automatic nitrogen gas adsorption instrument (Quantachrome, Boynton Beach, FL, USA), and the surface area of the UiO-66 MOF was obtained according to the multipoint BET (Brunauer, Emmett, Teller) method, while the average pore size and pore volume were performed by the BJH (Brunauer, Emmett, Teller) method.

Synthesis of UiO-66

UiO-66 was synthesized according to literature with minor modification.[32] As the chemical structure of UiO-66 has been widely reported in the literature we encourage the readers to read the references[35,36] to obtain a more detailed elucidation of its chemical structure. For the solution 1, five mmol of $ZrOCl_2.8H_2O$ was dissolved in 50.0 mL of DMF and 8.0 mL of concentrated HCl under magnetic stirring for 20 min, while solution 2 consisted of the dissolution of 7.0 mmol of terephthalic acid in 100.0 mL of DMF under magnetic stirring for 20 min, both at room temperature. Afterwards, solutions 1 and 2 were mixed and kept in an oven at 80 ºC for 21 h. After complete crystallization, the resulting material was filtered and washed with DMF to remove all residual terephthalic acid and dried at 80 ºC for 12 h. This material was named UiO-66 (DMF).

In order to avoid UiO-66 pores/channels blocking by DMF, the MOF was calcined in a porcelain capsule with heating ramp of 1º min^{-1} at 250 ºC for DMF removal. This material was then named UiO-66 (calcined).

On-line preconcentration of Cd^{2+} procedure coupled to TS-FF-AAS by the micro-packed column flow solid-phase extraction method

Preconcentration of Cd^{2+} using the flow injection system coupled to TS-FF-AAS was performed by percolating 10.0 mL of sample (buffered to pH 8.0 using 0.05 mol L^{-1} phosphate buffer) through a cylindrical mini-column (length 1.5 cm and an internal diameter of 5.0 mm) made of polypropylene packed with 20.0 mg of UiO-66 MOF, at a flow rate of 10.0 mL min^{-1}. After this step, the elution was performed by switching the injector to the elution position, using 1.0 mol L^{-1} HCl as eluent at a flow rate of 1.0 mL min^{-1}, where the desorbed Cd^{2+} ions were transported towards TS-FF-AAS detector. Pipette tips were inserted at each extremity of the cylindrical mini-column and pieces of cotton tissue were used to avoid losses of UiO-66 during preconcentration and elution steps.

Sample preparation

The tap and mineral water samples were obtained from the Chemistry Department of State University of Londrina and local supermarkets, respectively, while the physiological sample (NaCl 0.9% m/v) was acquired at a local drugstore. Lake sample was collected with amber glass bottle from Igapó Lake, located in Londrina (Brazil), and acidified with concentrated nitric acid until pH 2.0 to prevent the growth of microorganisms. The Igapó Lake water sample was filtered under vacuum using 0.45 μm cellulose acetate membrane and stored in freezer until analysis. Before use, an appropriate amount of a stock solution of phosphate buffer (1.0 mol L^{-1}) at pH 8.0 was diluted in the samples to obtain a final buffer concentration of 0.05 mol L^{-1}. For all samples, the analyses were carried out in triplicate.

Results and Discussion

Characterization of the UiO-66 adsorbent

X-ray diffraction patterns of UiO-66 (calcined) and UiO-66 (DMF) are depicted in Figure 1. As one can see, the diffractogram shows a typical crystalline structure of UiO-66 formed by clusters of octacoordinated zirconium ($ZrO_4(OH)_4$), in which the triangular faces of the Zr_6 octahedron are alternatively constituted by μ_3-O and μ_3-OH groups, and each cluster is connected to 12 other clusters via terephthalate ligands, in a face-centered cubic structure.[37] The appearance of distinctive peaks at 2θ = 7.33, 8.48, 12.03, and 25.67º indicates that UiO-66 was well synthesized without any sign of impurity in its crystalline structure.[38,39] Additionally, the calcined UiO-66 showed preserved crystalline structure, although with higher peak intensity.

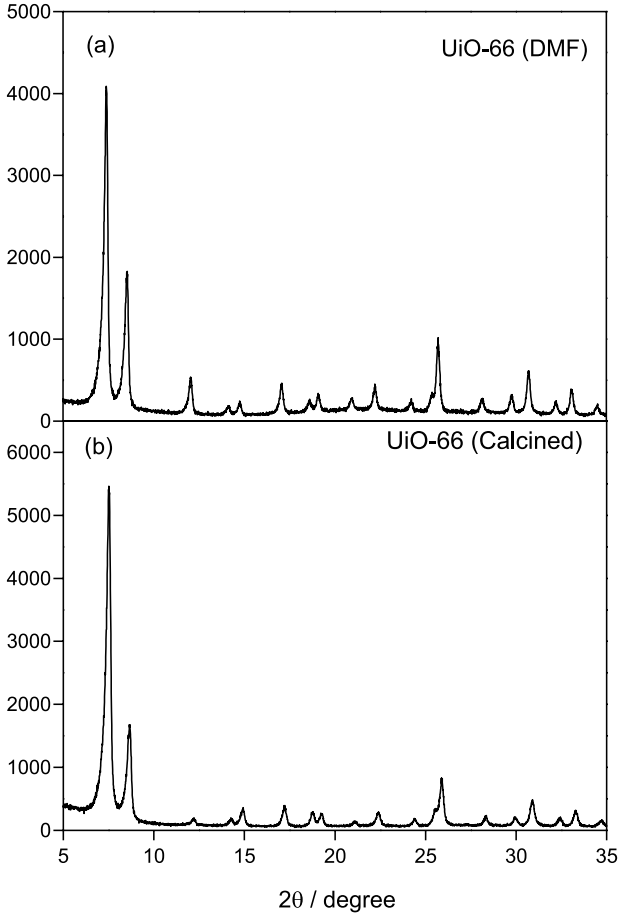

Figure 1. XRD patterns of the UiO-66 (a) synthesized in DMF and (b) after calcination.

The FTIR spectra of UiO-66 are shown in Figure 2. The bands at around 1398 and 1662 cm^{-1} can be attributed to the symmetric stretching of carboxylate groups whereas the band at 1574 cm^{-1} can be ascribed to its asymmetric stretching.[40-42] The band at 741 cm^{-1} is attributed to C–H vibration of the aromatic ring[42,43] and the bands at the region of 666 and 484 cm^{-1} are originated from O–Zr–O vibration.[40] The presence of low intensity bands at 2932 and 2858 cm^{-1} observed in the UiO-66 (DMF) spectrum can be ascribed to the symmetric/asymmetric stretching of C–H bonds of the adsorbed DMF molecules, which it is not observed in the UiO-66 (calcined) spectrum. This indicates that the total removal of the solvent was efficient and unblocked the channels of the UiO-66 without damaging its structure, thus favoring its application as adsorbent in solid-phase extraction.

Figure 3 shows the SEM images of UiO-66 (calcined), where aggregates of small crystallites resulting from the

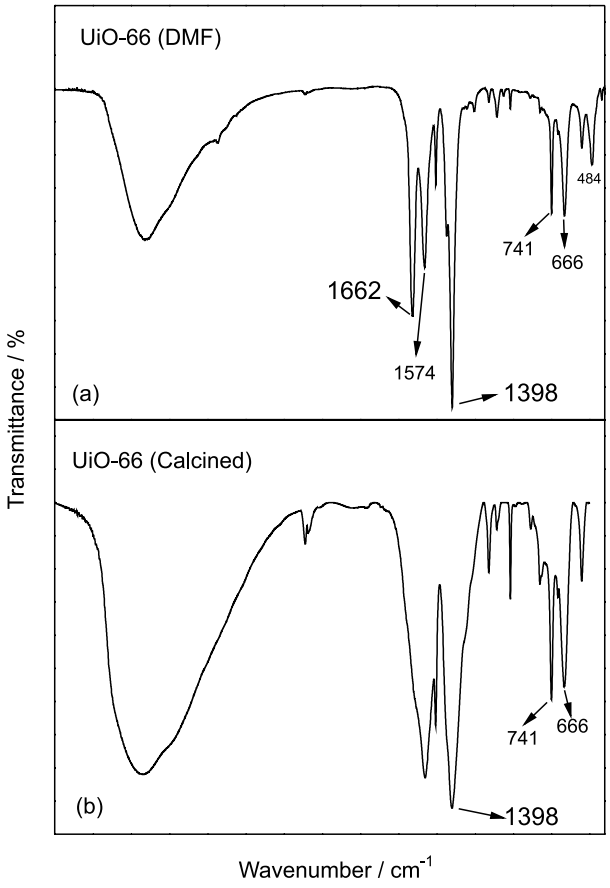

Figure 2. FTIR (KBr) spectra of UiO-66 (a) synthesized in DMF and (b) after calcination.

direct reaction of $ZrOCl_2$ with terephthalic acid were observed. In addition to the granular structure, a uniform particle size distribution was also observed, which is in agreement with studies reported in the literature.[44-48]

Raman absorption spectrum of the UiO-66 (calcined) is shown in Figure 4. The bands at 634 and 865 cm^{-1} are attributed to the ring C–H curvature vibrations out of plane, while the bands at 1146 and 1616 cm^{-1} are attributed to C=C modes of the benzene ring present in terephthalic acid. In addition, doublets at 1437 and 1452 cm^{-1} are usually assigned to units ν_{sym} ($C–O_2$) and ν_{asym} ($C–O_2$).[45,49-51]

In order to investigate the surface properties of the adsorbent UiO-66 (calcined) and UiO-66 (DMF), the N_2 adsorption-desorption isotherms were carried out and are shown in Figure 5, while the textural data obtained are arranged in Table 1.

As shown in Figure 5, both isotherms are of type 1, where the adsorption occurs with relatively low pressure, indicating the microporosity of the material. The BET surface area of UiO-66 (DMF) and UiO-66 (calcined) were found to be 1262 and 1562 $m^2\ g^{-1}$ with total pore volumes of 0.810 and 0.772 $cm^3\ g^{-1}$, respectively. This small increase in the surface area of UiO-66 (calcined) in relation to UiO-66 (DMF) is attributed to the removal of the solvent from the micropores by thermal activation, which might favor the adsorption capacity of material. Also, the average pore diameter confirms that the material is microporous, since it is lower than 2 nm.[43,52]

In order to evaluate the chemical stability of the UiO-66 after calcination and its crystalline structure, XRD patterns were assessed at different pH values. This study is of great importance, since cadmium preconcentration is carried out under basic medium and the elution is performed with diluted mineral acid. For this task, 100 mg of UiO-66 calcined was kept in contact with solutions at pH 1.0, 2.9, 5.8 and 8.0 during 48 h and, afterwards, the samples were filtrated under vacuum and dried at 90 ºC for 12 h.

As can be seen in Figure 6a, the XRD patterns show no crystalline structure failure when the UiO-66 is kept in solutions at pH 2.9, 5.8, and 8.0, thereby showing resistance to alkaline medium and slight acid medium. On the other hand, with the increase in the acidity of the

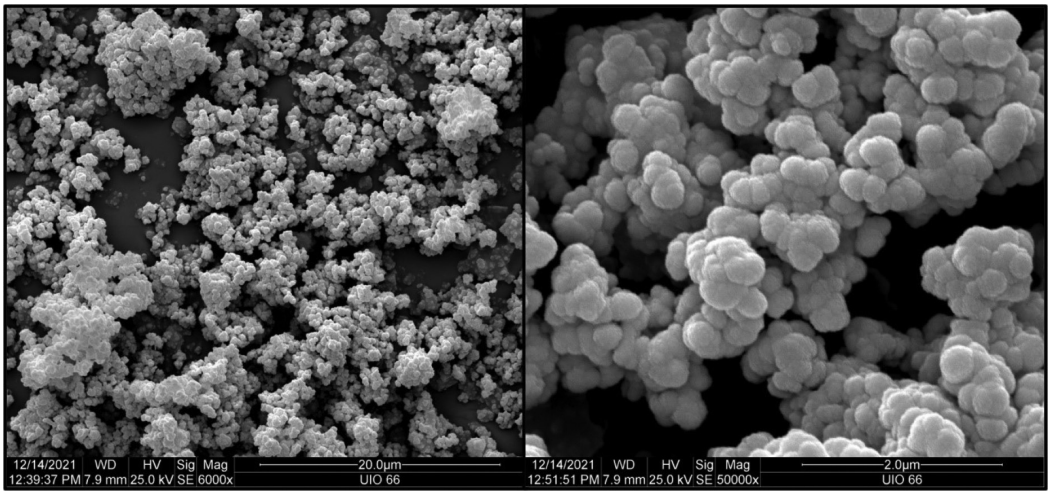

Figure 3. SEM images of UiO-66 (calcined).

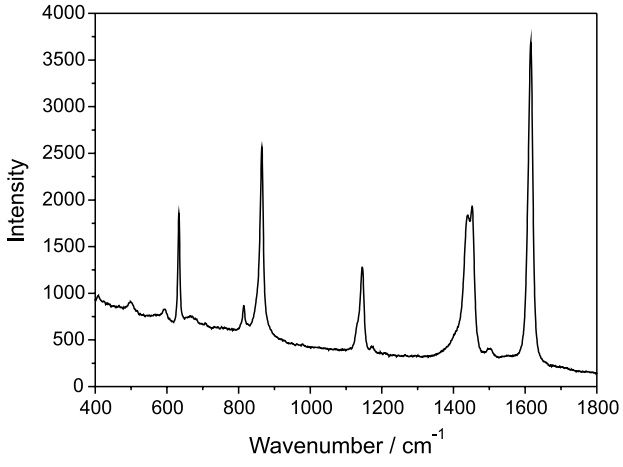

Figure 4. Raman spectrum of UiO-66 (calcined).

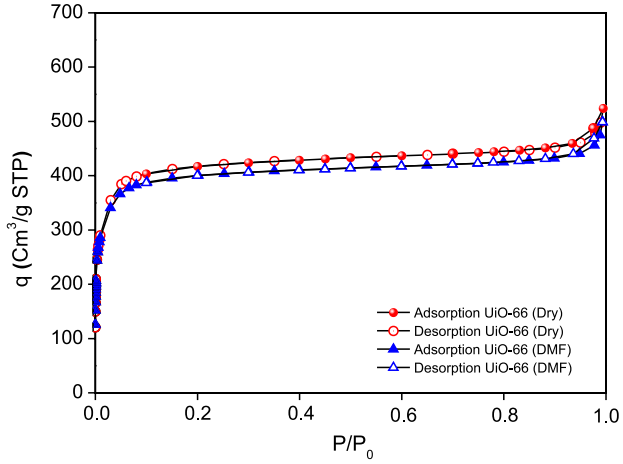

Figure 5. N_2 adsorption-desorption isotherms of the UiO-66 (calcined) and UiO-66.

medium (pH 1.0), a change in crystallinity patterns was observed, suggesting a partial degradation of the crystal structure (Figure 6b), evaluated mainly by the change in the peak area referring to the diffraction angle at $2\theta = 7.5°$.[53,54] Despite this finding, one should note that this study was carried out by keeping the UiO-66 in contact with highly acid solution for 48 h, which is a quite different condition from the one used in the flow preconcentration system, where the contact time of UiO-66 with acid at the elution step is much lower. For this reason, the chemical stability of UiO-66 was herein considered highly satisfactory, since only one mini-column was used through all method development, including the application in real samples, without decreasing the adsorption capacity.

Optimization of the on-line micro-packed column solid-phase procedure for cadmium preconcentration

For the optimization of the preconcentration procedure, only the UiO-66 (calcined) adsorbent was evaluated, thus it is going to be referred only by UiO-66 from this point. Preliminary studies regarding the amount (20 and 50 mg) of UiO-66 packed into the mini-column were carried out to evaluate possible leakages due to resulting pressure and the analytical performance in terms of preconcentration (data not shown). The use of 20 mg of adsorbent provided better results regarding the mini-column performance and stability, thus this value was chosen for further experiments. In addition, HCl was herein chosen instead of HNO_3 as eluent once the last one has oxidant properties, which would imply in a decrease of chemical stability of UiO-66. Also, metallic chlorides are more volatiles and, therefore, more suitable for the TS-FF-AAS technique, since the temperature inside the metallic tube is around 800-900 ºC. Other factors that play an important role in the preconcentration procedure, including preconcentration flow rate, eluent concentration, buffer concentration and sample pH, were evaluated from a full 2^4 factorial design. The levels of factors and the analytical responses (absorbance as peak height) are shown in Table 2. The experiments were carried out in triplicate by loading 10.0 mL of standard solution of cadmium at 5.0 µg L^{-1}.

The significance of factors on the preconcentration system was assessed from the Pareto chart (Figure 7) using a confidence level of 95%.

According to Pareto chart, sample pH and eluent concentration (EC) were the most significant factors at their higher levels. It is known that binding/interaction sites of MOF can be stablished between metallic ions and the clusters, as well as by the functional groups of chelating agents. Lewis acid-base interactions are considered as the most common adsorption mechanism between metallic ions and MOF.[55] The functional groups containing oxygen in the structure of UiO-66 from the organic ligands act as Lewis bases and strongly interact with cationic species

Table 1. Textural parameters for the UiO-66 with DMF and after calcination obtained from N_2 adsorption/desorption isotherms

Material	BET		
	Surface area / ($m^2 g^{-1}$)	Total pore volume / ($cm^3 g^{-1}$)	Average pore diameter / nm
UiO-66 (DMF)	1262 ± 23	0.810	0.372
UiO-66 (calcined)	1562 ± 10	0.772	0.378

DMF: *N*,*N*-dimethylformamide; BET: Brunauer, Emmett, Teller.

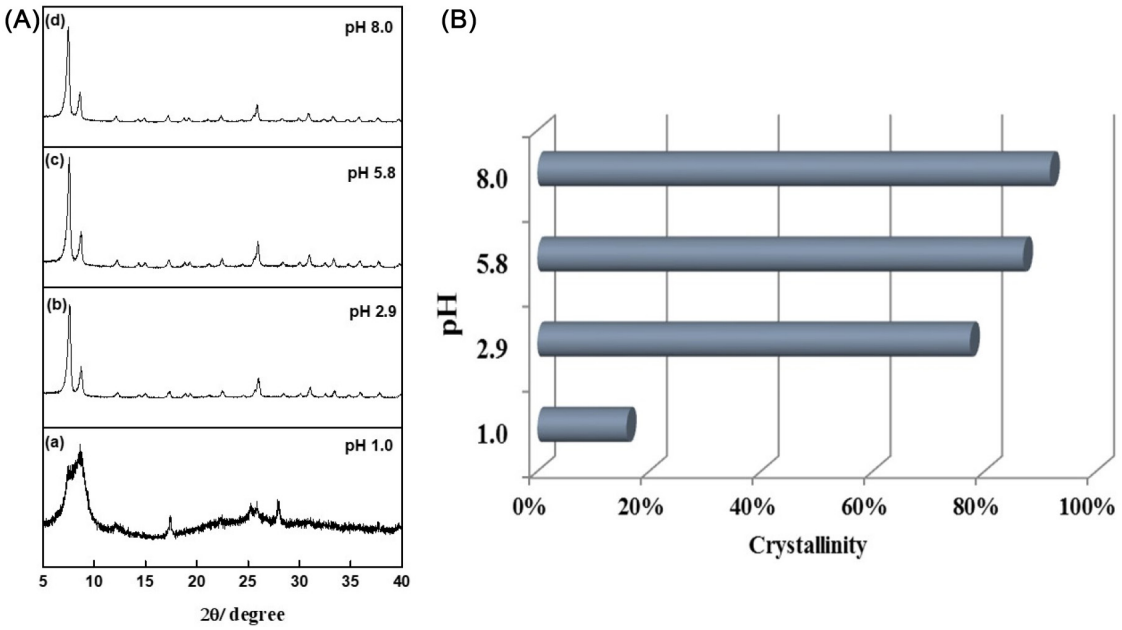

Figure 6. (A) XRD patterns and (B) crystallinity indicator of UiO-66 (calcined) adsorbent after being kept for 48 h in solutions at different pHs.

Table 2. Factors, levels, and analytical responses from the full 2^4 factorial design

Factor			Levels	
			Low (−)	High (+)
Preconcentration flow rate (PFR) / (mL min^{-1})			5.00	10.00
Buffer concentration[a] (BC) / (mol L^{-1})			0.05	0.10
pH			6.00	8.00
Eluent concentration (EC) / (mol L^{-1})			0.50	1.00
PFR	BC	pH	EC	Average ± SD
+	+	+	+	0.71 ± 0.06
+	+	+	−	0.65 ± 0.09
−	+	+	+	0.89 ± 0.02
−	+	+	−	0.93 ± 0.04
+	−	+	+	0.69 ± 0.07
+	−	+	−	0.66 ± 0.05
−	−	+	+	0.79 ± 0.00
−	−	+	−	0.93 ± 0.03
+	+	−	+	0.47 ± 0.09
+	+	−	−	0.84 ± 0.02
−	+	−	+	0.83 ± 0.06
−	+	−	−	0.35 ± 0.03
+	−	−	+	0.73 ± 0.12
+	−	−	−	0.47 ± 0.03
−	−	−	+	0.56 ± 0.06
−	−	−	−	0.52 ± 0.10

[a]Phosphate buffer solution. SD: standard deviation from analysis carried out in triplicate.

acting as Lewis acids, such as Cd^{2+}. Therefore, the positive standardized effect estimated for pH (3.63) indicates that higher analytical signal was observed at pH 8.0 due to the deprotonation of the functional groups that act as chelating binding sites for Cd^{2+} ions adsorption on the MOF.

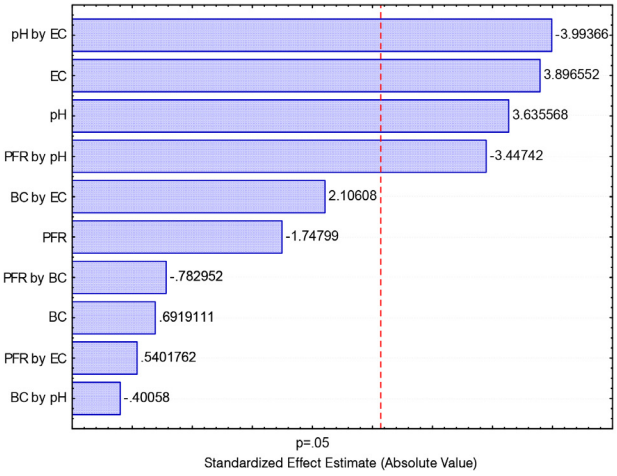

Figure 7. Pareto chart obtained from the full 2^4 factorial design. EC: eluent concentration (mol L^{-1}), BC: buffer concentration (mol L^{-1}) and PFR: preconcentration flow rate (mL min^{-1}).

The eluent concentration (EC) effect also presented positive standardized effect estimated (3.89), thereby indicating that, for lower concentrations, the desorption of cadmium from the UiO-66 is incomplete, which leads to memory effect during further preconcentration and elution steps. It is important to stress out that the interaction effect of pH and EC has a negative and significant standardized effect estimated of –3.99, which suggests that for a final simultaneous optimization, the influence of pH at its higher level is more pronounced when using lower EC and the other way around is also true. Such result can most likely be explained because, at high EC, there is a residual concentration of acid into the mini-column, in which the buffer solution has not enough buffering capacity to kept

constant the pH in the first milliliters of sample loading in the mini-column. Therefore, more complex experimental designs such as the Doehlert matrix could not be performed due to the memory effect drawbacks. Also, the memory effect could also be observed when building the analytical curve. In this sense, the best conditions were herein established as 1.0 mol L^{-1} HCl as eluent and samples at pH 8.0 and

Regarding the preconcentration flow rate (PFR), even using high levels (5.0 and 10.0 mL min^{-1}), no influence on the analytical response was observed, which clearly indicates a fast mass transfer kinetics of cadmium towards the UiO-66. Thus, in order to obtain a high sample throughput to the method, the preconcentration flow rate of 10.0 mL min^{-1} was chosen as the best condition. Buffer concentration (BC) within experimental domain did not feature any influence on analytical response and, thus, the lower concentration of 0.05 mol L^{-1} was adopted, aiming at lower consumption of reagent, as well as cost of analysis.

Effect of potentially interfering ions in the on-line micro-packed column solid-phase preconcentration of cadmium

Selectivity of the preconcentration method was evaluated through cadmium preconcentration of in the presence of potential interfering ions, such as Pb^{2+}, Hg^{2+}, Fe^{2+}, Co^{2+}, Cu^{2+}, Ni^{2+}, Zn^{2+}, Mg^{2+} or Ca^{2+}, which might be present in different types of water samples. For this task, binary solutions containing different ratios of analyte to interferent were subjected to the proposed method, where the Cd^{2+} concentration was fixed at 5.0 µg L^{-1}. The analytical signal of binary solution was then compared to a solution containing only 5.0 µg L^{-1} of Cd^{2+}, and the other ion was considered a potential interferent at certain concentration when a relative error of ± 10% in the analytical signal was obtained. Therefore, the degree of tolerance (µg L^{-1}), which is the high concentration that a potentially interfering ions can be present in the solution without interfering the preconcentration of cadmium, is shown in Table 3.

Even in the presence of high concentration for some metals, no interference in the cadmium preconcentration was observed, which might be attributed to high surface area of UiO-66. Therefore, the proposed method shows potentiality for an interference-free water samples analysis.

Analytical features and application of the proposed method for cadmium determination in water samples

As can be seen in Figure 8, the dynamic linear range of the proposed method was obtained within the concentration range of 0.10 to 8.00 µg L^{-1} with linear

Table 3. Tolerable concentration of potentially interfering ions on preconcentration of cadmium

Potentially interfering ions	Tolerable concentration / (µg L^{-1})	Recovery / %
Pb^{2+}	5.00	96.2
Hg^{2+}	5.00	96.0
Fe^{2+}	25.00	91.2
Co^{2+}	50.00	102.9
Cu^{2+}	50.00	102.9
Ni^{2+}	50.00	103.5
Zn^{2+}	50.00	98.9
Mg^{2+}	500.00	105.3
Ca^{2+}	500.00	102.3

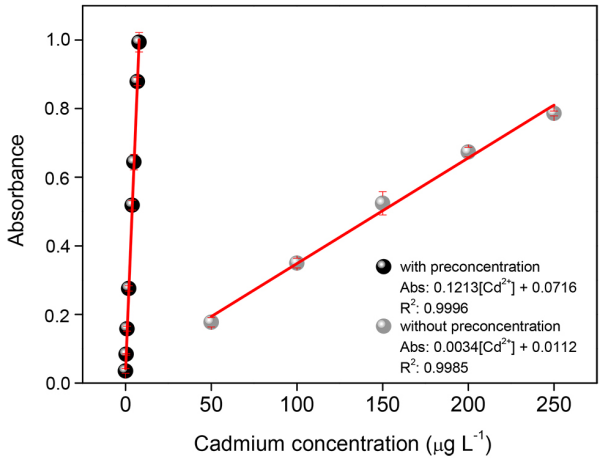

Figure 8. Analytical curves obtained with and without preconception step in TS-FF-AAS system under optimized conditions.

equation Abs = 0.1213[Cd^{2+}] + 0.0716, and determination coefficient of R^2 = 0.9996. For the measurements without preconcentration step, the linearity was within the concentration range of 50.00 to 250.00 µg L^{-1}, Abs = 0.0034[Cd^{2+}] + 0.0112 (R^2 = 0.9985). The preconcentration factor (PF) was determined as the ratio of the slopes of the analytical curves built with and without preconcentration step. Thus, PF obtained was 35.7. For 10.0 mL of sample, the limit of detection (LOD) of 0.03 µg L^{-1} and the limit of quantification (LOQ) of 0.10 µg L^{-1}, were defined according to International Union of Pure and Applied Chemistry (IUPAC) recommendations,[56] as 3std/m and 10std/m, respectively, where std is the standard deviation of 10 determinations of the analytical blank and m is the slope of the analytical curve. The concentration efficiency (CE), defined as the preconcentration factor obtained by operating the preconcentration procedure for 1 min, and the consumption index (CI), defined as the sample volume required to reach a unit of PF, were found to be 0.595 min^{-1}

Table 4. Comparison of the proposed method with recent studies reported in the literature to determine Cd^{2+} ions using on-line preconcentration coupled to TS-FF-AAS

Preconcentration method or adsorbent	Sample volume / mL	Chelating agent or precipitant agent	LOD / (μg L^{-1})	Eluent	PF	Reference
Hybrid imprinted polymer	10	–	0.03	HCl/ethanol	14.0	57
Nanocomposite based on MWCNTs and polyvinyl pyridine	8.8	–	0.03	HCl	19.5	58
Precipitation-dissolution in a knotted reactor	4.0	NH_3	0.04	HNO_3	34.0	59
Fullerene	1.5	APDC	0.10	ethanol	11	60
Polyurethane foam	2.0	DDTP	0.12	ethanol	5.2	61
Avocado seed activated carbon	10	–	0.12	HCl	10.7	62
UiO-66	10	–	0.03	HCl	35.7	this work

LOD: limit of detection; PF: preconcentration factor; MWCNTs: multiwalled carbon nanotubes; APDC: ammonium pyrrolidine dithiocarbamate; DDTP: diethyl dithiophosphate ammonium salt.

and 0.280 mL, respectively. The sample throughput of proposed method was 11 h^{-1}, considering the sample loading of 10.0 mL at a flow rate of 10.0 mL min^{-1}. The intra-day precision of the method, calculated for 10 consecutive measurements of standard solutions of Cd^{2+} at 1.0, 5.0 and 7.0 μg L^{-1} were found to be, respectively, 3.69; 0.64 and 0.13% (relative standard deviation), whereas the inter-day precision (two different days) for the same concentrations of Cd^{2+} was found to be 4.64; 2.86 and 0.54%, respectively.

Analytical methods involving on-line preconcentration coupled to TS-FF-AAS were compared to the proposed method (Table 4). The developed method proved to be highly efficient due to satisfactory sample consumption, high preconcentration factor and low limit of detection. In addition, the method is more environmentally-friendly and inexpensive to be carried out than those that makes use of fullerene and polyurethane foam due to the absence of toxic chelating agent during the pre-concentration flow system. Compared to hybrid imprinted polymer and the nanocomposite based on multiwalled carbon nanotubes (MWCNTs) and polyvinyl pyridine, the synthesis of UiO-66 is easier and inexpensive to be performed. Although the method that explores the precipitation-dissolution in a knotted reactor (KR) features satisfactory analytical features, it makes use of two peristaltic pumps and a standard rotary injection valve, in which naturally makes the method more expensive.

The accuracy of the method was attested by determining Cd^{2+} in different types of water samples followed by spiking known amounts of cadmium. The results are shown in Table 5.

The recoveries values varied from 92.0 to 111.9%, confirming the reliability of the proposed method for preconcentration and determination of Cd^{2+} ions in water samples with different matrix compositions.

Table 5. Application of the developed method in water samples and evaluation of recovery tests

Sample	Amount added of Cd^{2+} / (μg L^{-1})	Amount determined of Cd^{2+} / (μg L^{-1})	Recovery / %
Tap water	0.00	< LOD	–
	1.00	1.03 ± 0.03	103.3
	5.00	5.47 ± 0.01	109.3
	8.00	7.56 ± 0.01	94.4
Saline water	0.00	< LOD	–
	1.00	1.01 ± 0.02	100.6
	5.00	4.81 ± 0.01	96.2
	8.00	8.63 ± 0.01	107.8
Mineral water	0.00	0.30 ± 0.01	–
	1.00	1.27 ± 0.01	97.4
	5.00	5.10 ± 0.00	96.2
	8.00	7.64 ± 0.02	92.0
Lake water	0.00	< LOD	–
	1.00	1.12 ± 0.03	111.9
	5.00	5.47 ± 0.04	109.3
	8.00	7.45 ± 0.01	93.1

LOD: limit of detection. Numbers are mean concentration values ± SD (standard deviation) of (n = 3).

Conclusions

The performance of UiO-66 as adsorbent for cadmium preconcentration in an on-line micro-packed column procedure coupled to TS-FF-AAS was evaluated for the first time. The use of UiO-66 attends the requirements of green analytical chemistry in the flow system since no organic solvents and toxic chelating agents were used. Apart from these features, the synthesis of UiO-66, when compared to other adsorbents previously used for cadmium

preconcentration coupled to TS-FF-AAS, is easier and inexpensive to be performed. In terms of analytical features, the proposed method presents very low limit of detection, high preconcentration factor, low sample consumption, high reusability of UiO-66, since only one mini-column was used through all the method development, and absence of matrix effect for different types of water samples.

Supplementary Information

Supplementary data are available free of charge at http://jbcs.sbq.org.br as PDF file.

Acknowledgments

The authors acknowledge the financial support and fellowships of CAPES/Araucária Foundation No. 13/2018 - Post doctoral Fellowship, Coordenação de Aperfeiçoamento de Nível Superior (CAPES) finance code 001, Conselho Nacional de Desenvolvimento Científico e Tecnológico (CNPq) (grant No. 307432/2017-3), and Instituto Nacional de Ciência e Tecnologia de Bioanalítica (INCT) (FAPESP grant No. 2014/50867-3 and CNPq grant No. 465389/2014-7).

Author Contributions

Ana Carla R. Carneiro and Paula M. dos Santos developed the analytical method; Joziane G. Meneguin and Andrelson W. Rinaldi performed the synthesis and characterization of UiO-66; Marcela Z. Corazza and Maiyara Carolyne Prete participated in writing-original draft preparation and César Ricardo T. Tarley participated in conceptualization, funding acquisition and writing-original draft preparation.

References

1. Wang, X.; Xu, Y.; Li, Y.; Li, Y.; Li, Z.; Zhang, W.; Zou, X.; Shi, J.; Huang, X.; Liu, C.; Li, W.; *Food Chem.* **2021**, *357*, 129762.
2. United States Environmental Protection Agency (USEPA); *National Primary Drinking Water*, 2009, available at https://www.epa.gov/sites/production/files/2016-06/documents/npwdr_complete_table.pdf, accessed in March 2022.
3. World Health Organization (WHO); *Guidelines for Drinking-Water Quality*, 2017, available at http://apps.who.int/iris/bitstream/handle/10665/254637/9789241549950-eng.pdf;jsessionid=7C8A6ECE3B8ED11815030ACD748091E4?sequence=1, accessed in March 2022.
4. Ministério da Saúde; Portaria GM/MS No. 888, de 4 de maio de 2021, Altera o Anexo XX da Portaria de Consolidação GM/MS No. 5, de 28 de setembro de 2017, para Dispor sobre os *Procedimentos de Controle e de Vigilância da Qualidade da Água para Consumo Humano e seu Padrão de Potabilidade*; Diário Oficial da União (DOU), Brasília, No. 85, de 07/05/2021, p. 127, available at https://www.in.gov.br/en/web/dou/-/portaria-gm/ms-n-888-de-4-de-maio-de-2021-318461562, accessed in March 2022.
5. Corazza, M. Z.; dos Santos, P. M.; Segatelli, M. G.; Pereira, A. C.; Tarley, C. R. T.; *Quim. Nova* **2020**, *43*, 1086.
6. Dias, F. S.; Guarino, M. E. P. A.; Costa Pereira, A. L.; Pedra, P. P.; Bezerra, M. A.; Marchetti, S. G.; *Microchem. J.* **2019**, *146*, 1095.
7. de Almeida, F. G.; Ferreira, M. P.; Segatelli, M. G.; Beal, A.; Spinosa, W. A.; Cajamarca, F. A. S.; Tarley, C. R. T.; *React. Funct. Polym.* **2021**, *164*, 104934.
8. Welz, B.; Sperling, M.; *Atomic Absorption Spectrometry*, 3rd ed.; Wiley-VCH: Weinheim, 1999.
9. Demirtaş, İ.; Bakırdere, S.; Ataman, O. Y.; *Talanta* **2015**, *138*, 218.
10. Gáspár, A.; Berndt, H.; *Spectrochim. Acta, Part B* **2000**, *55*, 587.
11. Behbahani, M.; Veisi, A.; Omidi, F.; Noghrehabadi, A.; Esrafili, A.; Ebrahimi, M. H.; *Appl. Organomet. Chem.* **2018**, *32*, e4134.
12. Rezaee, M.; Khalilian, F.; *Quim. Nova* **2016**, *39*, 167.
13. Diniz, K. M.; Tarley, C. R. T.; *Microchem. J.* **2015**, *123*, 185.
14. Lemes, L. F. R.; Tarley, C. R. T.; *Food Chem.* **2021**, *357*, 129695.
15. dos Santos, W. N. L.; Costa, J. L. O.; Araujo, R. G. O.; de Jesus, D. S.; Costa, A. C. S.; *J. Hazard. Mater.* **2006**, *137*, 1357.
16. Tarley, C. R. T.; Scheel, G. L.; Ribeiro, E. S.; Zappielo, C. D.; Suquila, F. A. C.; *J. Braz. Chem. Soc.* **2018**, *29*, 1225.
17. Tiwari, S.; Sharma, N.; Saxena, R.; *New J. Chem.* **2017**, *41*, 5034.
18. Pourjavid, M. R.; Arabieh, M.; Yousefi, S. R.; Jamali, M. R.; Rezaee, M.; Hosseini, M. H.; Sehat, A. A.; *Mater. Sci. Eng., C* **2015**, *47*, 114.
19. Rocío-Bautista, P.; Taima-Mancera, I.; Pasán, J.; Pino, V.; *Separations* **2019**, *6*, 33.
20. Vu, H. D.; Nguyen, L.-H.; Nguyen, T. D.; Nguyen, H. B.; Nguyen, T. L.; Tran, D. L.; *Ionics* **2015**, *21*, 571.
21. Frem, R. C. G.; Arroyos, G.; Flor, J. B. S.; Alves, R. C.; Lucena, G. N.; da Silva, C. M.; Coura, M. F.; *Quim. Nova* **2018**, *41*, 1178.
22. Dai, X.; Jia, X.; Zhao, P.; Wang, T.; Wang, J.; Huang, P.; He, L.; Hou, X.; *Talanta* **2016**, *154*, 581.
23. Płotka-Wasylka, J.; Szczepańska, N.; de la Guardia, M.; Namieśnik, J.; *TrAC, Trends Anal. Chem.* **2016**, *77*, 23.
24. Rocío-Bautista, P.; González-Hernández, P.; Pino, V.; Pasán, J.; Afonso, A. M.; *TrAC, Trends Anal. Chem.* **2017**, *90*, 114.
25. Chen, Y.; Bai, X.; Ye, Z.; *Nanomaterials* **2020**, *10*, 1481.
26. Hu, B.; He, M.; Chen, B.; *Anal. Bioanal. Chem.* **2015**, *407*, 2685.
27. Esmaeilzadeh, M.; *New J. Chem.* **2019**, *43*, 4929.

28. Zhou, Y.-Y.; Yan, X.-P.; Kim, K.-N.; Wang, S.-W.; Liu, M.-G.; *J. Chromatogr. A* **2006**, *1116*, 172.
29. Yang, X.-Q.; Yang, C.-X.; Yan, X.-P.; *J. Chromatogr. A* **2013**, *1304*, 28.
30. Ahmed, A.; Forster, M.; Clowes, R.; Myers, P.; Zhang, H.; *Chem. Commun.* **2014**, *50*, 14314.
31. He, Q.; Chen, Q.; Lü, M.; Liu, X.; *Chin. J. Chem. Eng.* **2014**, *22*, 1285.
32. Katz, M. J.; Brown, Z. J.; Colón, Y. J.; Siu, P. W.; Scheidt, K. A.; Snurr, R. Q.; Hupp, J. T.; Farha, O. K.; *Chem. Commun.* **2013**, *49*, 9449.
33. Mondloch, J. E.; Katz, M. J.; Planas, N.; Semrouni, D.; Gagliardi, L.; Hupp, J. T.; Farha, O. K.; *Chem. Commun.* **2014**, *50*, 8944.
34. Ru, J.; Wang, X.; Wang, F.; Cui, X.; Du, X.; Lu, X.; *Ecotoxicol. Environ. Saf.* **2021**, *208*, 111577.
35. de Lima, H. H. C.; da Silva, C. T. P.; Kupfer, V. L.; Rinaldi, J. C.; Kioshima, E. S.; Mandelli, D.; Guilherme, M. R.; Rinaldi, A. W.; *Carbohydr. Polym.* **2021**, *251*, 116977.
36. Winarta, J.; Shan, B.; Mcintyre, S. M.; Ye, L.; Wang, C.; Liu, J.; Mu, B.; *Cryst. Growth Des.* **2020**, *20*, 1347.
37. Cavka, J. H.; Jakobsen, S.; Olsbye, U.; Guillou, N.; Lamberti, C.; Bordiga, S.; Lillerud, K. P.; *J. Am. Chem. Soc.* **2008**, *130*, 13850.
38. Ahmadijokani, F.; Mohammadkhani, R.; Ahmadipouya, S.; Shokrgozar, A.; Rezakazemi, M.; Molavi, H.; Aminabhavi, T. M.; Arjmand, M.; *Chem. Eng. J.* **2020**, *399*, 125346.
39. Morcos, G. S.; Ibrahim, A. A.; El-Sayed, M. M. H.; El-Shall, M. S.; *J. Environ. Chem. Eng.* **2021**, *9*, 105191.
40. Chen, S.; Yan, J.; Li, J.; Lu, D.; *Microchem. J.* **2019**, *147*, 232.
41. Ragon, F.; Campo, B.; Yang, Q.; Martineau, C.; Wiersum, A. D.; Lago, A.; Guillerm, V.; Hemsley, C.; Eubank, J. F.; Vishnuvarthan, M.; Taulelle, F.; Horcajada, P.; Vimont, A.; Llewellyn, P. L.; Daturi, M.; Devautour-Vinot, S.; Maurin, G.; Serre, C.; Devic, T.; Clet, G.; *J. Mater. Chem. A* **2015**, *3*, 3294.
42. Yan, Z.; Wu, M.; Hu, B.; Yao, M.; Zhang, L.; Lu, Q.; Pang, J.; *J. Chromatogr. A* **2018**, *1542*, 19.
43. Eltaweil, A. S.; Elshishini, H. M.; Ghatass, Z. F.; Elsubruiti, G. M.; *Powder Technol.* **2021**, *379*, 407.
44. Zhang, A.; Liu, B.; Liu, M.; Xie, Z.; Wang, D.; Feng, G.; *Sep. Purif. Technol.* **2021**, *270*, 118842.
45. Xu, H.; Zhu, J.; Cheng, Y.; Cai, D.; *Sens. Actuators, B* **2021**, *349*, 130793.
46. Zhou, L.; Zhang, X.; Chen, Y.; *Mater. Lett.* **2017**, *197*, 167.
47. Tang, X.; Luo, Y.; Zhang, Z.; Ding, W.; Liu, D.; Wang, J.; Guo, L.; Wen, M.; *Chem. Phys.* **2021**, *543*, 111093.
48. Qiu, J.; Feng, Y.; Zhang, X.; Jia, M.; Yao, J.; *J. Colloid Interface Sci.* **2017**, *499*, 151.
49. Roucan, M.; Kielmann, M.; Connon, S. J.; Bernhard, S. S. R.; Senge, M. O.; *Chem. Commun.* **2018**, *54*, 26.
50. He, L.; Dumée, L. F.; Liu, D.; Velleman, L.; She, F.; Banos, C.; Davies, J. B.; Kong, L.; *RSC Adv.* **2015**, *5*, 10707.
51. Cai, G.; Yin, Y.; Xia, D.; Chen, A. A.; Holoubek, J.; Scharf, J.; Yang, Y.; Koh, K. H.; Li, M.; Davies, D. M.; Mayer, M.; Han, T. H.; Meng, Y. S.; Pascal, T. A.; Chen, Z.; *Nat. Commun.* **2021**, *12*, 3395.
52. Rego, R. M.; Sriram, G.; Ajeya, K. V.; Jung, H.-Y.; Kurkuri, M. D.; Kigga, M.; *J. Hazard. Mater.* **2021**, *416*, 125941.
53. Kandiah, M.; Nilsen, M. H.; Usseglio, S.; Jakobsen, S.; Olsbye, U.; Tilset, M.; Larabi, C.; Quadrelli, E. A.; Bonino, F.; Lillerud, K. P.; *Chem. Mater.* **2010**, *22*, 6632.
54. Li, B.; Zhu, X.; Hu, K.; Li, Y.; Feng, J.; Shi, J.; Gu, J.; *J. Hazard. Mater.* **2016**, *302*, 57.
55. Vu, A. T.; Le, H. G.; Dao, C. D.; Dang, L. Q.; Nguyen, K. T.; Nguyen, Q. K.; Dang, P. T.; Tran, H. T. K.; Duong, Q. T.; Nguyen, T. V.; Lee, G. D.; *RSC Adv.* **2015**, *5*, 5261.
56. Long, G. L; Wineforddner, J. D.; *Anal. Chem*. **1993**, *55*, 712.
57. Tarley, C. R. T.; Corazza, M. Z.; de Oliveira, F. M.; Somera, B. F.; Nascentes, C. C.; Segatelli, M. G.; *Microchem. J.* **2017**, *131*, 57.
58. Tarley, C. R. T.; Diniz, K. M.; Cajamarca Suquila, F. A.; Segatelli, M. G.; *RSC Adv.* **2017**, *7*, 19296.
59. Wen, X.; Wu, P.; Xu, K.; Wang, J.; Hou, X.; *Microchem. J.* **2009**, *91*, 193.
60. Pereira, M. G.; Pereira-Filho, E. R.; Berndt, H.; Arruda, M. A. Z.; *Spectrochim. Acta, Part B* **2004**, *59*, 515.
61. Tarley, C. R. T.; Arruda, M. A. Z.; *Anal. Sci.* **2004**, *20*, 961.
62. Kudo, M. V. F.; de Oliveira, L. L. G.; Suquila, F. A. C.; de Almeida, F. G.; Segatelli, M. G.; Lima, É. C.; Dias, S. L. P.; Tarley, C. R. T.; *J. Braz. Chem. Soc.* **2020**, *31*, 100.

Submitted: October 31, 2021
Published online: March 17, 2022